Circulation Research

ORIGINAL RESEARCH

Spatiotemporal Control of Vascular $Ca_V1.2$ by $\alpha1_C$ S1928 Phosphorylation

Miguel Martín-Aragón Baudel; Victor A. Flores-Tamez; Junyoung Hong; Gopyreddy R. Reddy; Pauline Maillard; Abby E. Burns; Kwun Nok Mimi Man; Kent C. Sasse; Sean M. Ward; William A. Catterall; Donald M. Bers; Johannes W. Hell; Madeline Nieves-Cintrón*; Manuel F. Navedo*

BACKGROUND: L-type $Ca_V1.2$ channels undergo cooperative gating to regulate cell function, although mechanisms are unclear. This study tests the hypothesis that phosphorylation of the $Ca_V1.2$ pore-forming subunit $\alpha1_C$ at S1928 mediates vascular $Ca_V1.2$ cooperativity during diabetic hyperglycemia.

METHODS: A multiscale approach including patch-clamp electrophysiology, super-resolution nanoscopy, proximity ligation assay, calcium imaging, pressure myography, and Laser Speckle imaging was implemented to examine $Ca_V1.2$ cooperativity, $\alpha1_C$ clustering, myogenic tone, and blood flow in human and mouse arterial myocytes/vessels.

RESULTS: $Ca_V1.2$ activity and cooperative gating increase in arterial myocytes from patients with type 2 diabetes and type 1 diabetic mice, and in wild-type mouse arterial myocytes after elevating extracellular glucose. These changes were prevented in wild-type cells pre-exposed to a PKA inhibitor or cells from knock-in S1928A but not S1700A mice. In addition, $\alpha1_C$ clustering at the surface membrane of wild-type, but not wild-type cells pre-exposed to PKA or $P2Y_{11}$ inhibitors and S1928A arterial myocytes, was elevated upon hyperglycemia and diabetes. $Ca_V1.2$ spatial and gating remodeling correlated with enhanced arterial myocyte Ca^{2+} influx and contractility and *in vivo* reduction in arterial diameter and blood flow upon hyperglycemia and diabetes in wild-type but not S1928A cells/mice.

CONCLUSIONS: These results suggest that PKA-dependent S1928 phosphorylation promotes the spatial reorganization of vascular $\alpha1_C$ into "superclusters" upon hyperglycemia and diabetes. This triggers $Ca_V1.2$ activity and cooperativity, directly impacting vascular reactivity. The results may lay the foundation for developing therapeutics to correct $Ca_V1.2$ and arterial function during diabetic hyperglycemia.

GRAPHIC ABSTRACT: A graphic abstract is available for this article.

Key Words: cooperative gating ■ clustering ■ diabetes ■ hyperglycemia ■ vascular dysfunction

Meet the First Author, see p 950 | Editorial, see p 1034

L-type $Ca_V1.2$ channels play key roles in excitability, proliferation, gene expression, and muscle contraction.[1,2] A fundamental property of $Ca_V1.2$ channels is their intrinsic ability to functionally couple (eg, cooperative gating).[3–5] $Ca_V1.2$ cooperativity results in the amplification of Ca^{2+} influx.[4,6] This $Ca_V1.2$ gating mode regulates the function of cancer cells, cardiomyocytes, neurons, and arterial myocytes.[3,6–11] In arterial myocytes, $Ca_V1.2$ cooperative gating accounts for ≈50% of the total Ca^{2+} influx.[12] This is critical because Ca^{2+} influx via $Ca_V1.2$ couples the changes in membrane potential to arterial myocyte contraction,[13,14] thus influencing arterial diameter, blood flow, and blood pressure.[14] However, how $Ca_V1.2$ cooperative gating is regulated is poorly understood. Addressing this knowledge gap is important because of the impact this $Ca_V1.2$ gating modality has on cellular function.[4,6]

Correspondence to: Manuel F. Navedo, PhD, Department of Pharmacology, University of California Davis, One Shields Avenue, MED: PHARM Tupper 2419A, Davis, CA 95616. Email mfnavedo@ucdavis.edu; Madeline Nieves-Cintrón, PhD, Department of Pharmacology, University of California Davis, One Shields Avenue, MED: PHARM Tupper 2219A Davis, CA 95616. Email mcnieves@ucdavis.edu.
*M.N.-C. and M.F.N. contributed equally to this work.
Supplemental Material is available at https://www.ahajournals.org/doi/suppl/10.1161/CIRCRESAHA.122.321479.
For Sources of Funding and Disclosures, see page 1032.

Novelty and Significance

What Is Known?

- L-type $Ca_V1.2$ channels control cell excitability, proliferation, gene expression, and muscle contraction.
- $Ca_V1.2$ channels undergo cooperative gating that amplifies Ca^{2+} influx into cells, including arterial myocytes.
- Diabetic hyperglycemia augments vascular $Ca_V1.2$ activity leading to enhanced arterial myocyte contractility.

What New Information Does this Article Contribute?

- During diabetic hyperglycemia there is a spatial reorganization of the $Ca_V1.2$ pore-forming $\alpha1_C$ subunit into "superclusters" in association with increased frequency and strength of $Ca_V1.2$ cooperative gating in human and rodent arterial myocytes.
- Phosphorylation of $\alpha1_C$ at S1928, but not S1700, is essential for $\alpha1_C$ "superclustering" and $Ca_V1.2$ cooperative gating in arterial myocytes during diabetic hyperglycemia.
- S1928-dependent $\alpha1_C$ "superclustering" and $Ca_V1.2$ cooperative gating in diabetic hyperglycemia mediate enhanced arterial myocyte Ca^{2+} and contractility.

$Ca_V1.2$ channels are essential modulators of arterial myocyte contractility and, therefore, myogenic tone, blood flow, and blood pressure in health and disease. $Ca_V1.2$ regulation has been extensively studied, but recent evidence suggests that this modulation is more complicated than initially thought, with major tissue-specific differences. Results here highlight a previously unappreciated mechanism by which phosphorylation of a single amino acid – S1928 – in the $\alpha1_C$ subunit influences the spatial and temporal remodeling of vascular $Ca_V1.2$ channels to modulate vascular reactivity and blood flow in diabetic hyperglycemia. Similar observations in nondiabetic and diabetic human and rodent tissue provide additional translational relevance. Data also suggest that S1928 phosphorylation is a critical initial step underlying $Ca_V1.2$ cooperative gating by facilitating the superclustering of $\alpha1_C$ subunits, which may be a general mechanism altering $Ca_V1.2$ activity and vascular function in different pathological conditions. Results may also lay the foundation for conceptualizing the development of therapeutics that corrects $Ca_V1.2$ dysfunction rather than blocking its activity, which may decrease unwanted side effects.

Nonstandard Abbreviations and Acronyms

AC	adenylyl cyclase
CaM	calmodulin
cAMP	cyclic adenosine monophosphate
I_{Ba}	whole-cell barium current
nPo	number of channels X open probability
PLA	proximity ligation assay
PKA	protein kinase A
PKC	protein kinase C
S1700	serine 1700
S1928	serine1928
pS1928	S1928 phosphorylation
STZ	streptozotocin
TIRF	total internal reflection fluorescence
V_M	membrane potential
WT	wild type

$Ca_V1.2$ channels are multimeric protein complexes composed of pore-forming $\alpha1_C$ subunit and auxiliary β and $\alpha_2\delta$ subunits.[1,2] Prior studies suggested that the $\alpha1_C$ long carboxy-terminal is necessary for $Ca_V1.2$ cooperativity.[3,6,7] The model posits that physical interactions between the carboxy-terminal of 2 or more adjacent $\alpha1_C$ subunits facilitate $Ca_V1.2$ cooperative gating.[4] Emerging evidence suggests that $Ca_V1.2$ cooperativity can be stimulated by protein kinases.[3,4,15] These results lead to the hypotheses that $\alpha1_C$ subunits may form clusters that facilitate functional $\alpha1_C$ interactions and that phosphorylation of $\alpha1_C$ could be a key initial step inducing and promoting $\alpha1_C$ clustering and $Ca_V1.2$ cooperative gating. Our study is designed to test these possibilities.

$Ca_V1.2$ channel regulation has been the subject of extensive investigation. Different mechanisms have been proposed. For example, disinhibition of the $\alpha1_C$ subunit by phosphorylation-dependent removal of the small GTPase Rad from the cardiac $Ca_V1.2$ channel complex is necessary for β adrenergic regulation of channel activity.[16] Other studies have implicated direct $\alpha1_C$ phosphorylation at conserved phosphorylation sites, including phosphorylation at serine 1928 (S1928; Figure S1), by protein kinases in $Ca_V1.2$ regulation in cardiac cells, neurons, and arterial myocytes.[17–23] Intriguingly, recent reports showed that increased vascular $Ca_V1.2$ channel activity in response to elevated extracellular glucose (eg, hyperglycemia; HG) and diabetes is dependent on augmentation of S1928 phosphorylation (pS1928).[17,18,24–27] HG/diabetes-induced pS1928 was mediated by engagement of a signaling complex scaffolded by AKAP5 and involving the G_S-coupled $P2Y_{11}$ (human)/$P2Y_{11}$-like (murine) receptor, adenylyl cyclase 5 (AC5), and protein kinase A (PKA).[17,18,26,28] In this complex, the G_S-coupled $P2Y_{11}$

receptors are activated by extracellular nucleotides (eg, ATP) upon HG.[18] This leads to AC5 stimulation to produce a highly localized cAMP signal,[27] which activates a pool of PKA in close association to the $\alpha1_C$ subunit, increasing pS1928.[17] Although initial studies suggested that HG and diabetes could increase vascular $Ca_V1.2$ cooperativity,[29] whether pS1928 mediates this gating mode is unknown. Examining this possibility is important because it could identify pS1928 as a critical event mediating $Ca_V1.2$ cooperativity through the redistribution of $\alpha1_C$ into larger clusters, which may underlie alterations in vascular function during pathological conditions such as diabetic hyperglycemia.

Here, we examine pS1928 as a key initial step in controlling the spatial organization of $\alpha1_C$ subunits to facilitate vascular $Ca_V1.2$ cooperative gating during diabetic hyperglycemia. We present evidence in human and mouse arterial myocytes indicating that HG and diabetes promote the formation of larger $\alpha1_C$ clusters and increase the frequency and strength of vascular $Ca_V1.2$ cooperativity. Disruption of pS1928 in arterial myocytes from S1928A mice prevented the increase in $\alpha1_C$ clustering and $Ca_V1.2$ cooperative gating in response to HG and diabetes. The changes in vascular $Ca_V1.2$ channel spatial and gating mode upon HG and diabetes were correlated with increased arterial myocyte Ca^{2+} influx and contractility, resulting in a reduction in arterial diameter and blood flow in WT but not S1928A mice. Thus, we propose $\alpha1_C$ pS1928 as a rheostat of vascular $Ca_V1.2$ function and vascular reactivity and a "risk factor" for vascular complications during diabetic hyperglycemia.

METHODS

Data Availability

All data are included in the article and Supplemental Material file. MN-C and MFN had full access to all the data in the study and takes responsibility for its integrity and data analysis.

Detailed methodological information and a Resources Table can be found in the Supplemental Material file. Hierarchical "nested" analyses with appropriate statistical tests were performed.[30]

RESULTS

Increased $Ca_V1.2$ Clustering and Cooperativity in Cells of People With Diabetes

We examine $Ca_V1.2$ properties in arterial myocytes from male and female patients with and without type 2 diabetes (Table S1).[17,18,26,27,31] For this, we used cell-attached electrophysiology to record $Ca_V1.2$ channels undergoing single or cooperative openings.[32] $Ca_V1.2$ currents were evoked by 2-second voltage steps from −70 mV to −30 mV with Ca^{2+} as the charge carrier. Under these conditions, unitary $Ca_V1.2$ openings have amplitudes of ≈0.5 pA (Figures 1A, 1B).[3,6,33] Initial analysis confirmed elevated $Ca_V1.2$ channel activity (eg, nPo) in myocytes of people with diabetes (Figures 1A–1C, Table S2).[17] Open-time analysis was performed independently in unitary and cooperative events because $Ca_V1.2$ cooperativity may already show higher activity,[3,12] masking the diabetic effects. Data showed a slight yet significant increase in the unitary $Ca_V1.2$ open-time in myocytes of people with diabetes (Figure 1D, Table S2). The open-time for cooperative events was not different between groups but was comparable to the unitary open-time in cells of people with diabetes (Figure S1, Table S3). Closed-time analysis showed 2 components, which were shorter in cells of people with diabetes (Figure 1E, Table S2). Thus, an increased opening time and reduced stability of the closed-state may contribute to the elevated nPo in arterial myocytes of people with diabetes.

We also found increased channel availability (ie, likelihood of at least 1 event per sweep; Figure 1F, Table S2) and frequency of cooperative events (number of traces showing $Ca_V1.2$ openings produced by 2 or more channels; Figure 1G, Table S2) in myocytes of people with diabetes. $Ca_V1.2$ cooperativity was further quantified with a coupled Markov chain model to determine coupling strength (ie, κ).[3,34] This analysis found that $Ca_V1.2$ κ was elevated in cells of people with diabetes (Figure 1H, Table S2). These results suggest increased $Ca_V1.2$ channel activity and cooperativity in arterial myocytes of people with diabetes.

Enhanced $Ca_V1.2$ cooperativity in arterial myocytes of people with diabetes implies that $\alpha1_C$ subunits must come into close physical apposition (eg, larger clusters). To test this premise, super-resolution direct stochastic optical reconstruction microscopy nanoscopy in the total internal reflection fluorescence (TIRF) mode was performed in arterial myocytes with an $\alpha1_C$ antibody.[35,36] This approach detects $\alpha1_C$ clusters at/near the plasma membrane of arterial myocytes with a ≈15–20 nm lateral resolution.[17,18,26,27] The direct stochastic optical reconstruction microscopy-rendered maps revealed $\alpha1_C$ clusters of various sizes in arterial myocytes of people with and without diabetes (Figure 1I). We also found increased mean $\alpha1_C$ cluster size in cells of people with diabetes (Figures 1J, Table S2). No statistically significant difference was observed in $\alpha1_C$ cluster density between cells of people with and without diabetes (Figure 1K, Table S2). A nearest-neighbor interpolation analysis revealed that the mean number of $\alpha1_C$ clusters within a 250-nm radius of each cluster was augmented in cells of people with diabetes (3.6–5.2 clusters; Figure 1L, Table S2). These results suggest a spatial reorganization of plasma membrane $\alpha1_C$ subunits into larger clusters that may facilitate increased $Ca_V1.2$ channel activity and cooperativity in human arterial myocytes during diabetes.

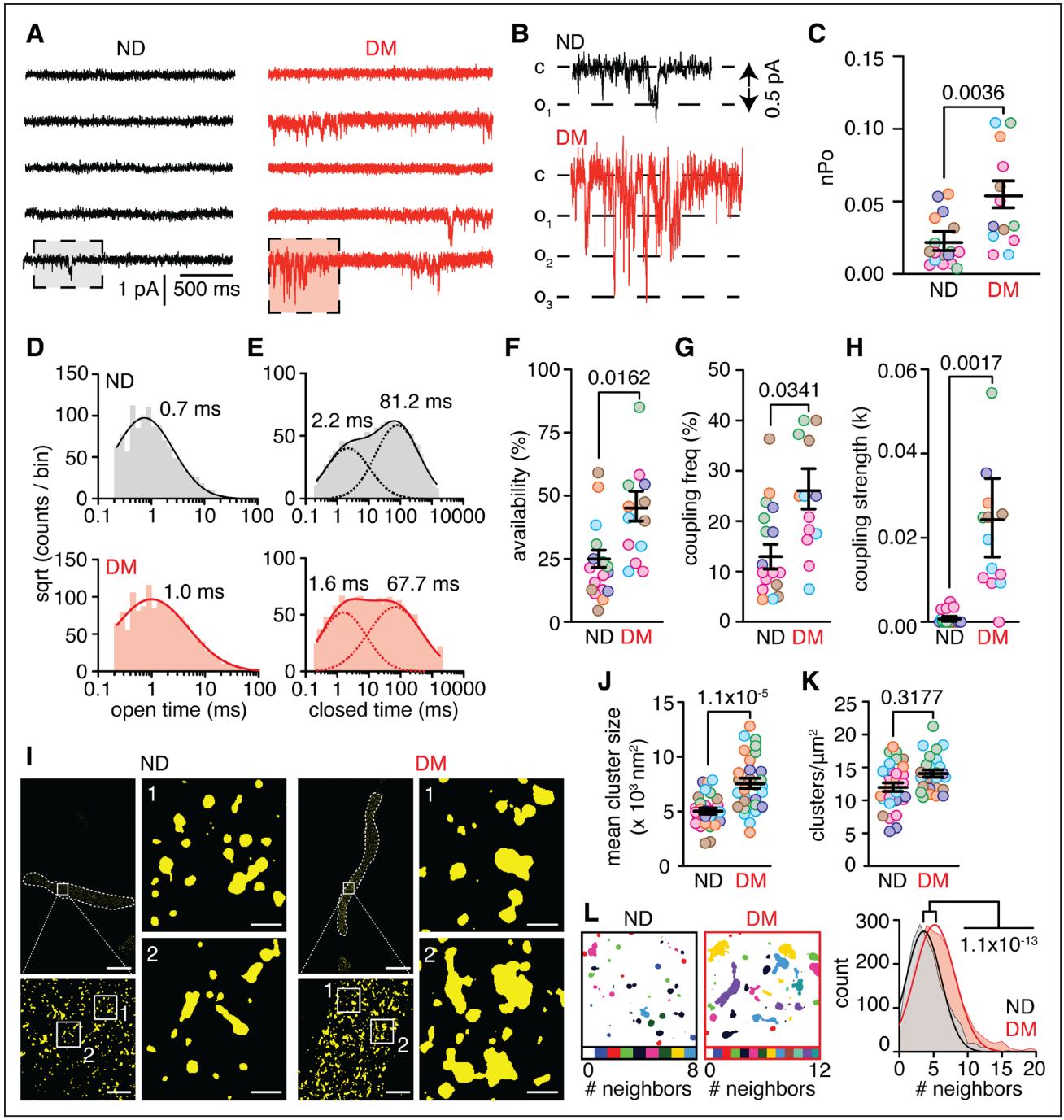

Figure 1. Increased $Ca_V1.2$ cooperativity and $\alpha1_C$ clustering in cells of diabetic patients.
A, Representative cell-attached recordings of arterial myocytes of people with diabetes mellitus (DM)] and without (ND) diabetes during a 2 s depolarizing step from −80 mV to −30 mV. **B**, Magnified areas from boxed areas in A, highlighting the closed (c) and unitary $Ca_V1.2$ opening levels (o_n). Summary data of (**C**) number of channels X open probability (nPo), unitary events (**D**) open-time and (**E**) closed-time histograms, (**F**) availability, (**G**) coupling frequency and (**H**) coupling strength (ND n=17 cells from 6 human samples; DM n=13 cells from 6 human samples). (**I**) Representative super-resolution total internal reflection fluorescence (TIRF) images of arterial myocytes labeled for $\alpha1_C$ subunits with 2 magnified areas showing cluster size and distribution in arterial myocytes from ND and DM samples (scale bars=10 µm→1 µm→0.2 µm). Amalgamated data for (**J**) cluster size and (**K**) cluster density. (**L**) Representative nearest-neighbor interpolation maps color-coded as a function of the number of neighbors within a 250 nm radius and summary data fitted with Gaussian curves (ND n=29 cells from 6 human samples; DM n=29 cells from 5 human samples). Data are mean±SEM. Significance was assessed with nested *t*-tests for most conditions. Open/closed-time histograms were fitted with 1 or 2 Gaussian components, and centroids for open-time histograms (**D**) were compared using an extra sum-of-squares F test (P=1.1×10^{-13}). *P* values within each panel and Table S2.

pS1928 Controls Ca$_V$1.2 Cooperativity and $\alpha 1_C$ Clustering Upon HG

Elevated blood glucose levels (ie, hyperglycemia; HG) is a major metabolic abnormality in diabetes. Prior studies suggested that HG increases Ca$_V$1.2 current density in human and mouse arterial myocytes, which is mediated by $\alpha 1_C$ pS1928.[17,18] Consistent with this, whole-cell electrophysiology using Ba^{2+} as charge carrier confirmed increased nifedipine-sensitive Ca$_V$1.2 current density (I_{Ba}) in mouse WT arterial myocytes when the extracellular glucose concentration was elevated from 10 mmol/L (control condition) to 20 mmol/L (HG) D-glucose (Figure S3A, Table S4). These D-glucose concentrations are similar to nonfasting glucose concentrations measured in nondiabetic and diabetic mice and have been extensively used to study glucose-mediated changes in murine arterial myocytes.[17,18,26,27,29,37–39] Glucose effects are not due to osmolarity changes, as 20 mmol/L L-glucose or 20 mmol/L mannitol did not potentiate I_{Ba} in arterial myocytes.[17,18,24,26,27] When the same experiments were repeated in arterial myocytes from a knockin mouse in which serine 1928 was mutated to alanine to prevent its phosphorylation (eg, S1928A mouse[40]), 20 mmol/L D-glucose did not elevate I_{Ba} (Figure S3A, Table S4). This lack of I_{Ba} response to HG in S1928A cells was not due to changes in total protein abundance of the $\alpha 1_C$ subunit (Figure S3B, Table S4) or Ca$_V$1.2 voltage dependency of activation or inactivation (measured as in Navedo et al study[41]) between WT and S1928A cells (Figure 2A, Table S5). 20 mmol/L D-glucose significantly leftward-shifted the Ca$_V$1.2 voltage dependency of activation (≈6 mV) but not inactivation in WT cells (Figure 2B, Table S5). No statistically significant difference in Ca$_V$1.2 voltage dependency of activation or inactivation to HG was detected in S1928A cells (Figure 2B, Table S5). These results confirm a key role for pS1928 in modulating I_{Ba} upon HG.

To test if pS1928 is necessary for HG-induced vascular Ca$_V$1.2 cooperativity, cell-attached electrophysiology (Ca^{2+} as charge carrier) was performed in WT and S1928A arterial myocytes exposed to 10 mmol/L and 20 mmol/L D-glucose. Data showed that 20 mmol/L D-glucose significantly increased Ca$_V$1.2 nPo in WT cells (Figures 2C–2E, Table S5). This effect was prevented in WT cells pre-treated with the PKA inhibitor rpcAMP (Figures S3C and 3D, Table S4) and S1928A myocytes (Figures 2C–2E, Table S5). Although the Ca$_V$1.2 nPo in S1928A cells seems lower compared with WT cells, this is not statistically different (P=0.1198; Table S5). Open-time analysis showed a slight yet significant increase in Ca$_V$1.2 unitary and cooperative open-times in WT but not in S1928A cells (Figures 2F–2G, Figures S3C–S3D, Tables S4–S5). Closed-time analysis showed 2 components in both WT and S1928A cells, with WT myocytes displaying a pronounced decrease in the long component from 54.6 ms to 9.1 ms upon 20 mmol/L D-glucose (Figure 2F, Table S5). The S1928A cells also showed a reduction in the long closed-time component, but not as pronounced as in WT cells (Figures 2F and 2G, Table S5). Further analysis found that Ca$_V$1.2 channel availability was higher in WT myocytes but not WT cells treated with rpcAMP or S1928A cells exposed to 20 mmol/L D-glucose (Figure 2H, Figure S3G, Tables S4 and S5). Quantification of Ca$_V$1.2 cooperative frequency and strength revealed a significant augmentation in both parameters upon 20 mmol/L D-glucose in WT myocytes, and these changes were prevented in WT cells treated with rpcAMP and S1928A cells (Figures 2I and 2J, Figures S3H and S3I, Tables S4 and S5). The lack of response of Ca$_V$1.2 channels in S1928A myocytes to HG is not due to impairment in the activation of the signaling pathway as 20 mmol/L D-glucose elevated cAMP levels, as measured with FRET biosensors,[42–44] to the same level in WT and S1928A myocytes (Figure S3J, Table S4). Results suggest that HG stimulates Ca$_V$1.2 cooperativity, which requires PKA-dependent pS1928 in arterial myocytes. Moreover, data suggest that enhanced Ca$_V$1.2 clustering upon HG is unlikely to make vascular Ca$_V$1.2 channels more susceptible to Ca^{2+}-dependent inactivation but rather induce them to be in a high nPo mode.[6,45]

We examined if HG alters the spatial organization of $\alpha 1_C$ and if $P2Y_{11}$, PKA, and pS1928 mediate such rearrangement. We implemented a 2-pronged approach using proximity ligation assay (PLA) and super-resolution imaging. We used a modified PLA validated by us and others to examine $\alpha 1_C$ oligomerization/clustering.[46,47] A similar modified PLA has been used to examine oligomerization/clustering of epidermal growth factor receptors and α-synuclein.[48,49] In our modified PLA, a single $\alpha 1_C$ monoclonal antibody is labeled with the PLUS or MINUS probe. Because the $\alpha 1_C$ monoclonal antibody binds to the same epitope, each $\alpha 1_C$ Plus or α_{1C} Minus probe binds to only 1 $\alpha 1_C$ subunit. A PLA signal is produced only if 2 independent $\alpha 1_C$ subunits are closer than 40 nm, allowing the detection of $\alpha 1_C$ oligomers/clusters (Figure S4A and Methods section). Experiments found a significant increase in PLA puncta/area to 20 mmol/L D-glucose in WT myocytes (Figure 3A, Table S6). This change was not observed in S1928A myocytes or WT cells pre-treated with the $P2Y_{11}$ receptor antagonist NF340 or the PKA inhibitor rpcAMP (Figure 3A, Figure S4B, Tables S6 and S7). The cell-wide PKA activator forskolin increased PLA puncta/area in WT cells to the same extent as 20 mmol/L D-glucose (Figure S4B, Table S7). No PLA puncta were observed when one of the primary antibody-probe was omitted (Figure S4C). These results suggest that HG induces $P2Y_{11}$/PKA-dependent pS1928, leading to an increase in α_{1C} oligomerization/clustering.

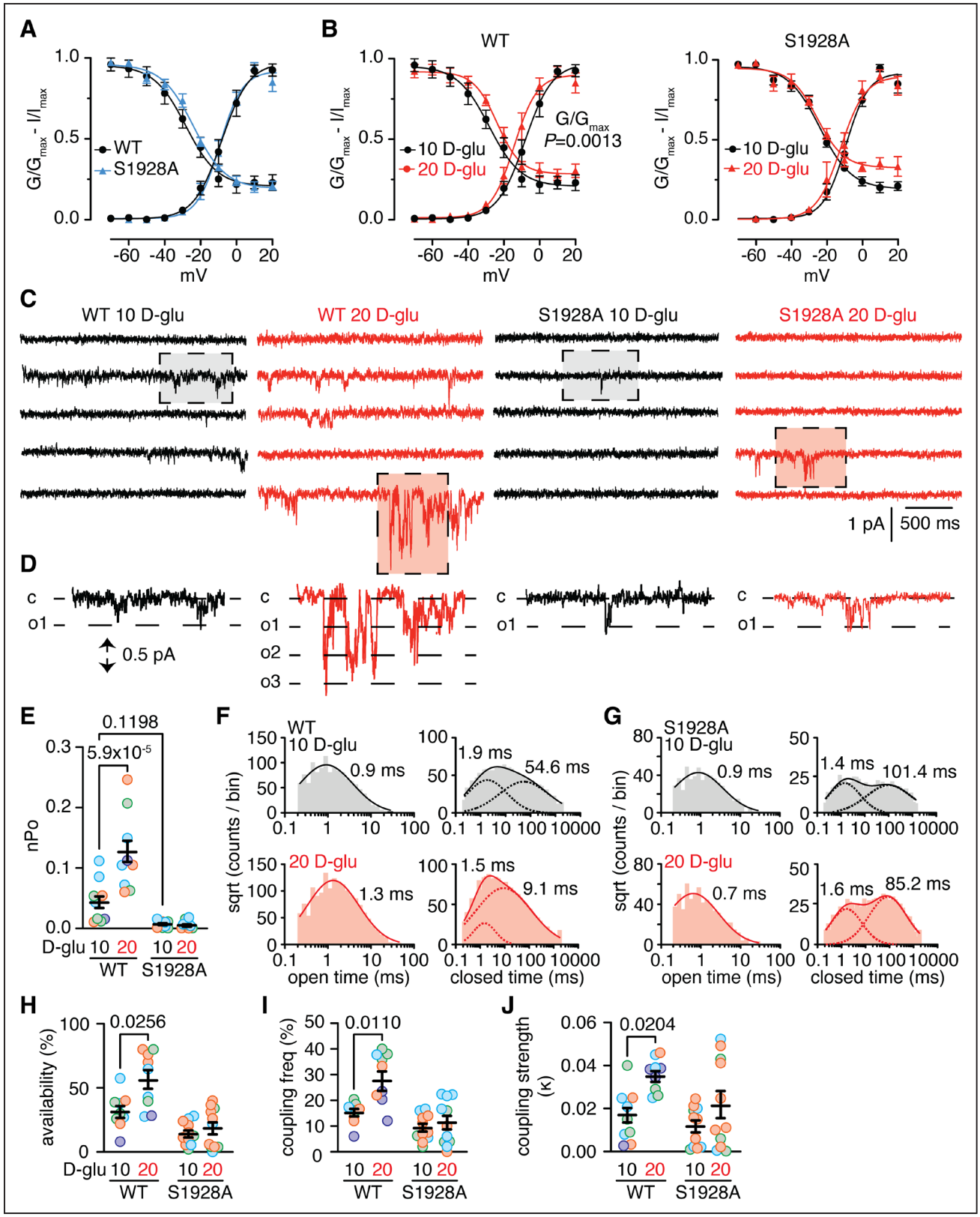

Figure 2. pS1928 controls $Ca_V1.2$ cooperative gating upon HG.

A, **B**, Voltage dependency of activation and steady-state inactivation fitted with a Boltzmann model from wild-type (WT) and S1928A arterial myocytes under control/10 mmol/L D-glucose conditions and 20 mmol/L D-glucose (WT: n=9 cells from 4 mice; S1928A: n=8 cells from 4 mice). **C**, Representative cell-attached recordings from WT and S1928A arterial myocytes during a 2 s depolarizing step from −80 mV to −30 mV upon 10 mmol/L and 20 mmol/L D-glucose. **D**, Magnified areas from boxed regions in C highlighting the closed (c) and unitary $Ca_V1.2$ opening levels (o_n). Summary data of (**E**) nPo, (**F**, **G**) unitary events open and closed-time histograms for WT and S1928A, (*Continued*)

Super-resolution nanoscopy showed increased $\alpha1_C$ cluster size at/near the plasma membrane of WT myocytes treated with 20 mmol/L D-glucose (Figures 3B and 3C, Table S6). This HG-induced spatial re-arrangement was not observed in WT cells pretreated with NF340 or rpcAMP or in S1928A cells (Figures 3B and 3C, Figure S4D, Tables S6 and S7). $\alpha1_C$ cluster density was not statistically different upon stimulation with 20 mmol/L D-glucose in WT and S1928A arterial myocytes (Figure 3D, Table S6). However, nearest-neighbor analysis found that 20 mmol/L D-glucose induced a significant increase in the number of neighbors within a 250-nm radius from each cluster in WT (5.9–7.0) but not S1928A (5.6–5.2) arterial myocytes (Figure 3E, Table S6). $\alpha1_C$ clusters were never observed in cells when the primary antibody was omitted (Figure S4C). These data support the premise that HG incites a spatial rearrangement of $\alpha1_C$ into larger clusters in arterial myocytes that are dependent on $P2Y_{11}$ and PKA activity, leading to pS1928. Larger $\alpha1_C$ clusters can then promote $Ca_V1.2$ cooperativity in arterial myocytes upon HG.

S1700 phosphorylation Is Not Required for HG-Induced $Ca_V1.2$ Regulation

The $\alpha1_C$ amino acid serine 1700 (S1700; Figure S2) has been implicated in PKA-dependent regulation of cardiac $Ca_V1.2$ channels.[22,50] To examine if S1700 phosphorylation is necessary for $Ca_V1.2$ regulation by HG, arterial myocytes from a knockin mouse expressing an $\alpha1_C$ subunit with serine 1700 mutated to alanine to prevent its phosphorylation (eg, S1700A[22]) were used. Whole-cell electrophysiology with step depolarization from −70 mV to +10 mV found that 20 mmol/L D-glucose significantly increased nifedipine-sensitive I_{Ba} (Figure 4A, Table S8). Single-channel data obtained by step depolarization from −80 mV to −30 mV with Ca^{2+} as the charge carrier revealed that 20 mmol/L D-glucose increased nPo, availability, and coupling frequency and strength (Figures 4B–4G, Table S8). Pressure myography in arteries pressurized to 60 mm Hg showed that 20 mmol/L D-glucose caused arterial constriction and increased myogenic tone (Figure 4H, Table S8). cAMP signal in response to HG was similar in S1700A compared with WT and S1928A cells (Figure S3J, Table S4). These results are comparable to WT arterial myocytes/arteries (see Figure 2)[17,18,26,27]. Data suggest that S1700 phosphorylation is not required for increased $Ca_V1.2$ function and myogenic tone upon HG.

pS1928 Controls Arterial Myocyte Ca^{2+} and Contractility Upon HG

We examined the physiological effects of pS1928-mediated increases in $\alpha1_C$ clustering and $Ca_V1.2$ cooperativity upon HG. In silico data suggested that HG could promote arterial myocyte membrane depolarization in WT and S1928A cells but that pS1928 was still necessary for HG-induced elevations in intracellular Ca^{2+} [51] To test these predictions, membrane potential (V_M) was measured in WT and S1928A arterial myocytes in response to 20 mmol/L D-glucose using the perforated whole-cell patch-clamp.[46] V_M was similar in WT (−58 ± 2 mV) and S1928A (−58 ± 3 mV) cells exposed to 10 mmol/L D-glucose (Figure 5A, Table S9). These V_M in isolated WT and S1928A cells are comparable to V_M previously reported using microelectrodes in WT arterial myocytes of pressurized arteries.[13,37] Exposure to 20 mmol/L D-glucose induced V_M depolarization to −46 ± 3 mV in WT and −47 ± 3 mV in S1928A cells (Figure 5A, Table S9), resulting in a comparable magnitude of depolarization (ΔV_M: −12 mV in WT and −11 mV in S1928A). A 60 mmol/L K^+ solution caused depolarization in WT (−14 ± 2 mV) and S1928A cells (−16 ± 2 mV) to comparable V_M and the expected Nernst equilibrium potential (Figure 5A, Table S9). These results confirm the in silico predictions experimentally that HG-induced V_M depolarization is not reliant on pS1928.

To test the prediction that pS1928 is necessary for HG-induced elevations in intracellular Ca^{2+} concentration ($[Ca^{2+}]_i$), arterial myocytes were loaded with the membrane-permeable fluorescent Ca^{2+} indicator fluo-4 AM. The fluorescent signal emanating from the cells was also used to track arterial myocyte length and assess contractility (Supplemental Materials).[52] 20 mmol/L D-glucose increased peak $[Ca^{2+}]_i$ with concomitant cell contraction in WT cells (Figure 5B, Table S9). Peak $[Ca^{2+}]_i$ and contractility were not statistically different upon 20 mmol/L L-glucose (Figure 5B, Table S9), suggesting that the 20 mmol/L D-glucose effects are not due to osmolarity factors.[17,18,26–28] In contrast, exposure of S1928A cells to 20 mmol/L D-glucose did not elevate peak $[Ca^{2+}]_i$ or caused contraction (Figure 5B, Table S9). These results uphold the in silico prediction that pS1928 is necessary for HG-induced increased $[Ca^{2+}]_i$, leading to arterial myocyte contraction.

To corroborate an in vivo physiological role for pS1928 upon HG, myogenic tone and blood flow were measured in cerebral arteries via a cranial window in anesthetized mice using Laser Speckle imaging.[26,27] The cranial

Figure 2 Continued. (**H**) availability, (**I**) coupling frequency and (**J**) coupling strength (WT n=9 cells from 4 mice; S1928A n=11 cells from 4 mice). Data are mean±SEM. Significance was assessed with extra sum-of-squares F test (**A**: V_{50}-activation P=0.5601, V_{50}-inactivation P=0.0989; **B**: WT V_{50}-activation P=0.0013, V_{50}-inactivation P=0.1067, S1928A V_{50}-activation P=0.1273, V_{50}- inactivation P=0.2640; **F**: P=0.0002 and **G**: P=0.0521) and nested two-way ANOVA (**E**: P=0.0007, **H**: P=0.0345, **I**: P=0.0314 and **J**: P=0.0280) with Bonferroni posthoc test for all conditions. Open/closed-time histograms were fitted with 1 or 2 Gaussian components, and centroids for open-time histograms were compared using an extra sum-of-squares F test (**F**: WT P=0.0002; **G**: S1928A P=0.0521). P values within each panel and Table S5.

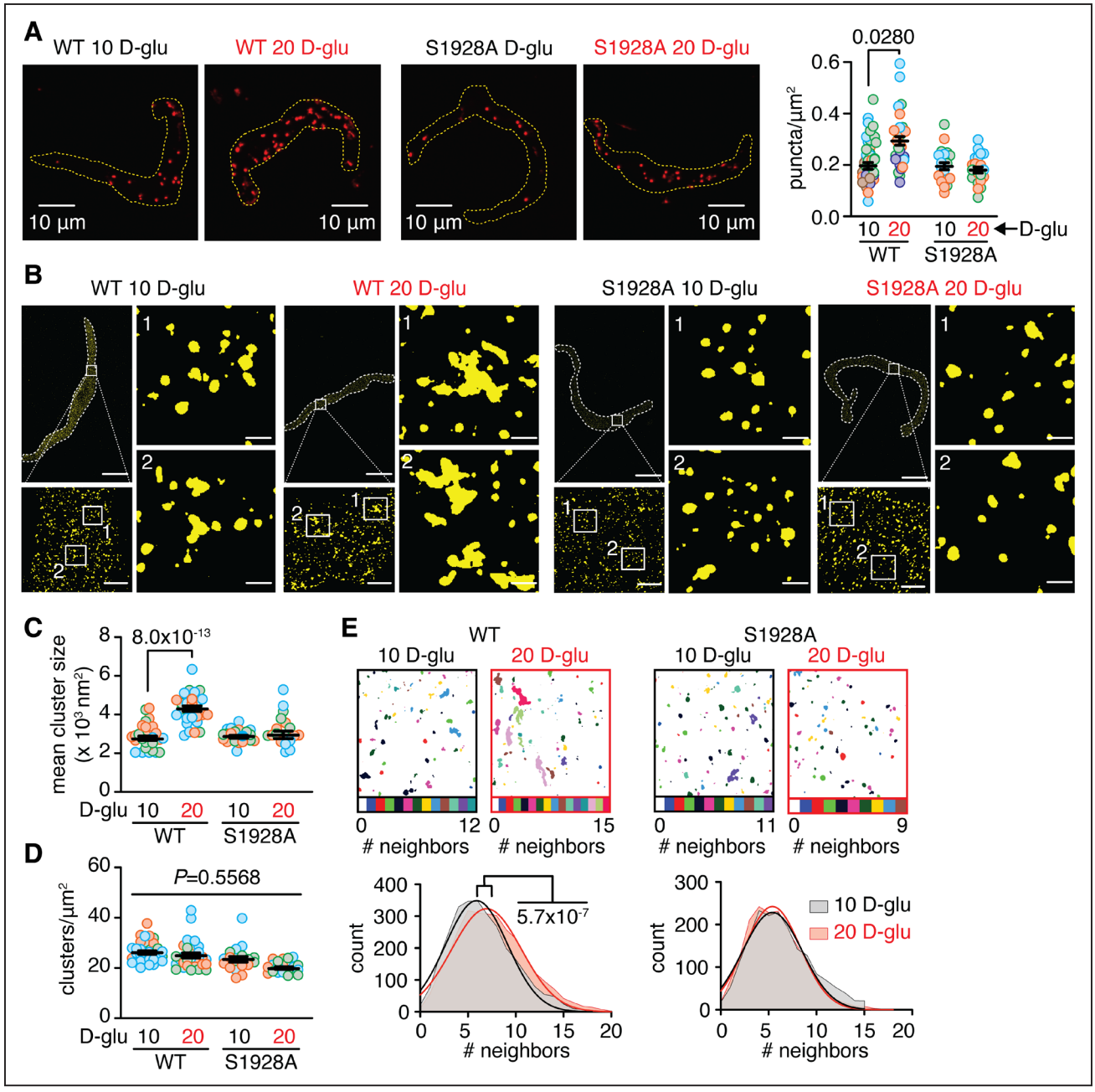

Figure 3. pS1928 mediates increased $\alpha 1_C$ clustering upon HG.
A, Representative images of proximity ligation assay (PLA) puncta of $\alpha 1_C$-$\alpha 1_C$ interactions from WT and S1928A myocytes upon 10 mmol/L and 20 mmol/L D-glucose. Dashed lines represent cells' footprints and summary puncta/µm² (WT 10 D-glu n=32 cells from 5 mice, 20 D-glu n=37 cells from 5 mice; S1928A 10 D-glu n=22 cells from 3 mice, 20 D-glu n=22 cells from 3 mice). **B**, Representative super-resolution TIRF images of arterial myocytes labeled for $\alpha 1_C$ with 2 magnified areas showing cluster size and distribution in WT and S1928A arterial myocytes (scale bars=10 µm→1 µm→ 0.2 µm). Amalgamated data for (**C**) cluster size and (**D**) cluster density. (**E**) Representative nearest-neighbor interpolation maps color-coded as a function of the number of neighbors within a 250-nm radius and frequency distribution fitted with Gaussian curves (WT 10 D-glu n=27 cells from 3 mice, 20 D-glu n=27 cells from 3 mice; S1928A 10 D-glu n=20 cells from 3 mice, 20 D-glu n=19 cells from 3 mice). Data are mean±SEM. Significance was assessed with nested 2-way ANOVA with Bonferroni post-hoc test (**A**: P=0.0281, **C**: P=8.0×10^{-13}, **D**: P=0.5568) and with extra sum-of-squares F test comparing centroids (**E**: WT P=5.7×10^{-7}, S1928A P=0.0703). P values within each panel and Table S6.

window was permeated with a control artificial cerebrospinal fluid solution (see Methods section) containing 10 mmol/L D-glucose to collect stable arterial diameter and blood flow. A vasodilatory mixture (see Methods section) was used to induce maximal dilation and calculate myogenic tone and normalized blood flow. Flooding the cranial window with 20 mmol/L D-glucose resulted in a reduction in arterial diameter, which translated into an increase in myogenic tone and a concomitant decrease in blood flow in WT but not S1928A mice (Figure 5C,

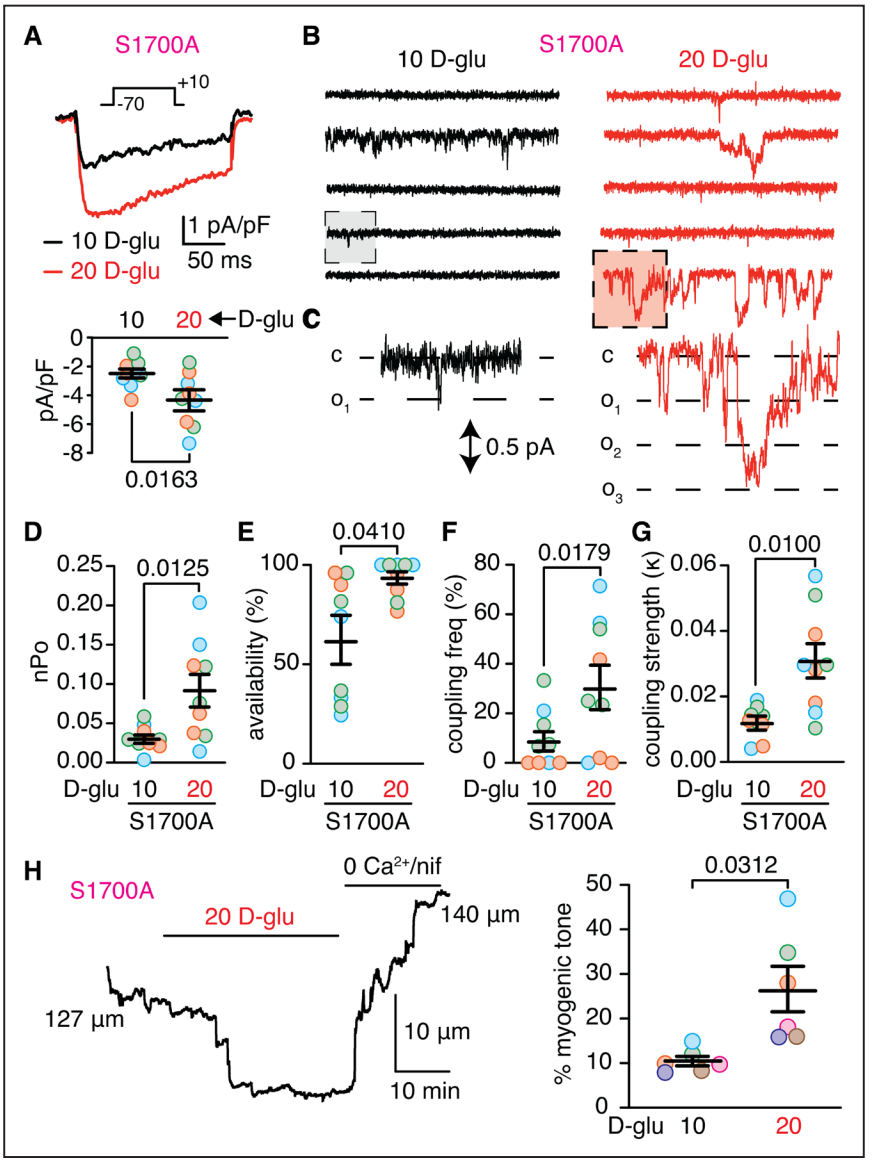

Figure 4. S1700 phosphorylation (pS1700) is not required for HG-induced CaV1.2 cooperative gating.
(**A**) Exemplary whole-cell nifedipine-sensitive I_{Ba} traces to a depolarizing step from −70 mV to +10 mV and amalgamated current density from WT and S1700A (n=9 cells from 3 mice). (**B**) Representative cell-attached recordings from WT and S1700A cerebral arterial myocytes during a 2 s depolarizing step from −80 mV to −30 mV upon 10 mmol/L and 20 mmol/L D-glucose. (**C**) Magnified areas from boxed regions in B highlighting the closed (c) and unitary Ca$_V$1.2 opening levels (o_n). Summary data of (**D**) nPo, (**E**) availability, (**F**) coupling frequency and (**G**) coupling strength (n=9 cells from 3 mice). **H**, Representative diameter recording, and summary percentage myogenic tone from S1700A cerebral arteries upon 10 mmol/L and 20 mmol/L D-glucose (n=6 arteries from 5 mice). Data are mean±SEM. Significance was assessed with nested *t*-test. *P* values within each panel and Table S8.

Table S9). These results suggest that HG-induced changes in cerebral artery myogenic tone and blood flow require pS1928.

pS1928 Underlies Increased Ca$_V$1.2 Clustering and Cooperativity in Diabetes

Considering the link between hyperglycemia and diabetes,[53,54] we examined if pS1928 is required for Ca$_V$1.2 structural and functional remodeling in arterial myocytes from a streptozotocin (STZ)-induced type 1 diabetic mouse model.[55] Age-matched WT and S1928A mice were injected with citrate buffers (sham) or STZ. Non-fasting blood glucose levels were elevated, and body weight was smaller in WT and S1928A STZ mice (Table S10).[27] A 10 mmol/L D-glucose solution was used to perform experiments in sham and STZ arteries and arterial myocytes from WT and S1928A mice.

The modified PLA assay (Figure S4A and[46,47]) showed that PLA puncta density was significantly elevated in WT but not S1928A, STZ arterial myocytes compared with WT/S1928A sham cells (Figure 6A, Table S11). No PLA

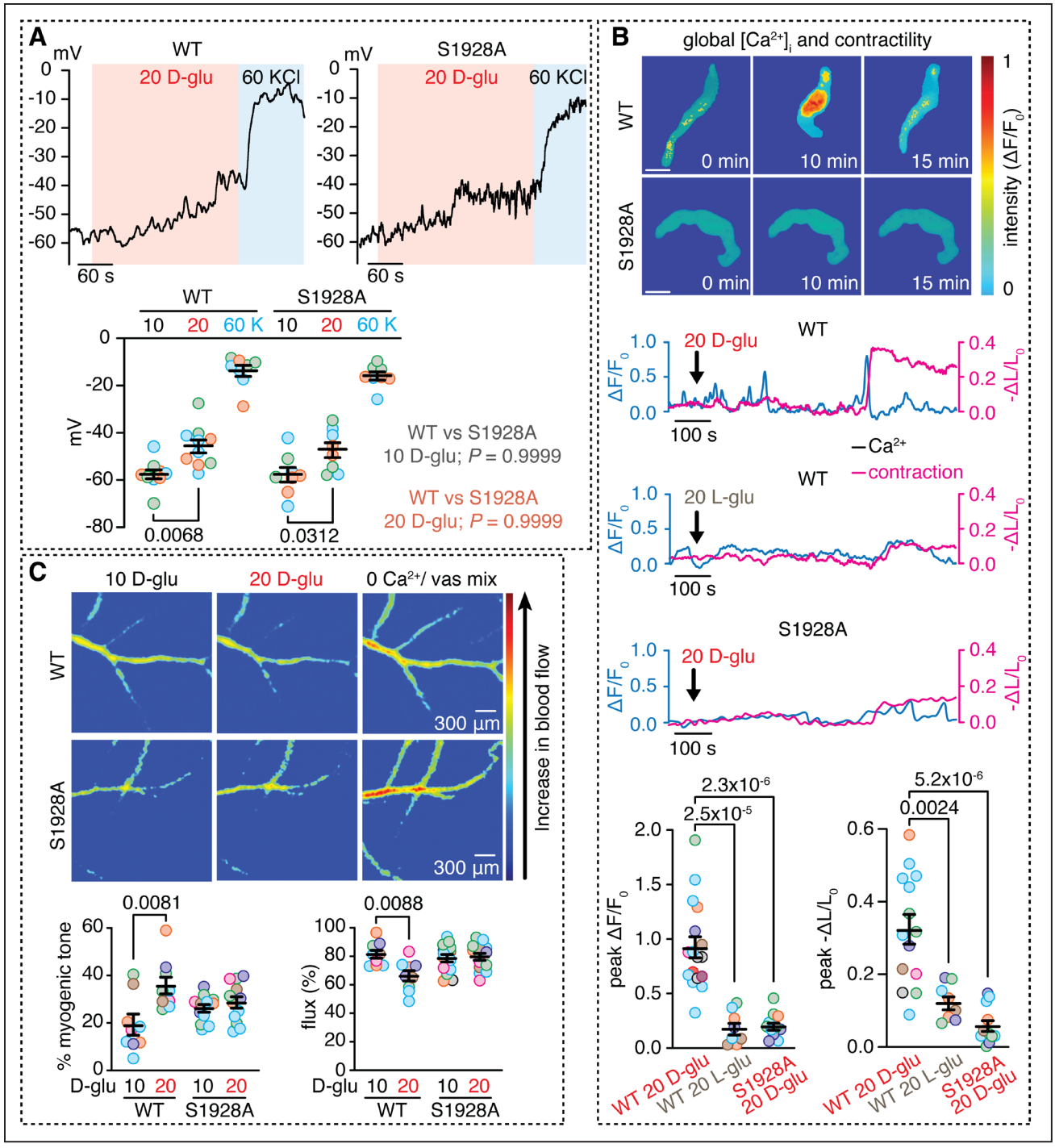

Figure 5. pS1928 is necessary for increased arterial myocyte Ca^{2+} and contractility upon HG.
A, Representative traces of perforated whole-cell recordings from WT and S1928A cerebral arterial myocytes in current-clamp mode with a gap-free protocol and summary data of V_m upon 10 mmol/L D-glu, 20 mmol/L D-glue and 60 mmol/L KCl (WT n=10 cells from 3 mice; S1928A n=8 cells from 3 mice). (**B**) Representative normalized pseudo-colored confocal images at different time points and resulting fluorescence (black) and cell length (red) traces of WT and S1928A cerebral arterial myocytes loaded with the fluorescent Ca^{2+} indicator fluo-4 AM. Summary data of peak $[Ca^{2+}]_i$ and cell length of WT and S1928A arterial myocytes upon 20 mmol/L D-glu or 20 mmol/L L-glu ($[Ca^{2+}]_i$: WT 20 mmol/L D-glu n=17 cells from 9 mice, 20 mmol/L L-glu n=8 cells from 5 mice; S1928A 20 mmol/L D-glu n=12 cells from 5 mice; cell length: WT 20 mmol/L D-glu n=14 cells from 6 mice, 20 mmol/L L-glu n=8 cells from 5 mice; S1928A 20 mmol/L D-glu n=12 cells. From 5 mice). (**C**) Representative pseudo-colored blood flow images of WT and S1928A cerebral pial arteries through a cranial window exposed to 10 mmol/L D-glu, 20 mmol/L D-glu or 0 Ca^{2+} + vasodilatory mix and summary data of myogenic tone and flux (WT n=9 arteries from 6 mice; S1928A n=12 arteries from 6 mice). Data are mean±SEM. Significance was assessed with nested 2-way ANOVA with Bonferroni post-hoc test (**A**: P=0.0141, **C**: P=0.0445) and nested ANOVA with a 3-level factor (**B**: $P=5.6\times10^{-7}$ for peak $\Delta F/F_0$ and $P=4.9$–10^{-6} for peak $\Delta L/L_0$). P values within each panel and Table S9.

ORIGINAL RESEARCH

signal was observed when the primary antibody was omitted (Figure S5A). Super-resolution imaging uncovered a significant increase in $\alpha1_C$ cluster size (Figures 6B and 6C, Table S11) and the number of neighbors within a 250 nm radius from each cluster (Figure 6D, Table S11) in WT STZ compared with WT and S1928A sham and STZ cells. Cluster density was similar in WT and S1928A sham and STZ cells (Figure S5B, Table S12). No signal was detected when the primary antibody was omitted (Figure S5C). These results suggest that diabetes rearranges $\alpha1_C$ into larger clusters in arterial myocytes and that pS1928 mediates this remodeling.

Correlating with the pS1928-dependent $\alpha1_C$ superclustering during diabetes, arterial myocytes from WT but not S1928A mice in STZ showed larger whole-cell nifedipine-sensitive I_{Ba} compared with sham (Figure S6A, Table S13). Moreover, single-channel recordings of $Ca_V1.2$ channels revealed that nPo, channel availability, and coupling frequency and strength were all elevated in WT STZ compared with WT sham arterial myocytes (Figures 7A–7E, Figure S6B, Table S14). The unitary open-time was increased in WT STZ cells (Figure 7F and Table S14). Although the cooperative open time was not different in WT sham and STZ cells (Figure S6C, Table S13), the increase in the frequency of $Ca_V1.2$ cooperativity in WT diabetic cells will still result in greater Ca^{2+} influx.[12] The closed-time analysis showed that the frequency of events with the short closed-time component increased in WT STZ arterial myocytes (Figure 7F, Table S14), thus suggesting a destabilization of the channel closed-state. These diabetes-induced alterations in $Ca_V1.2$ properties were prevented/ameliorated in S1928A STZ compared

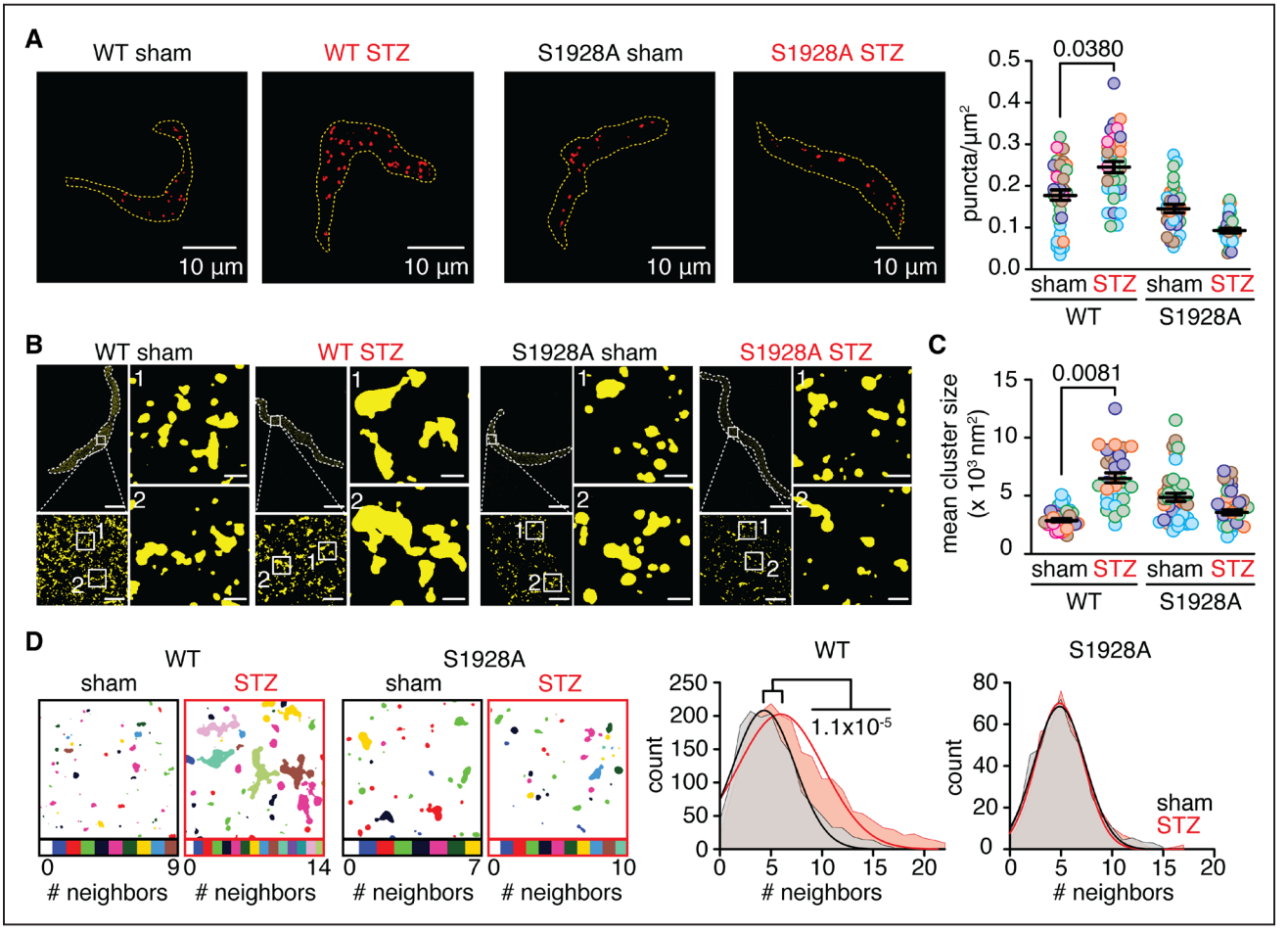

Figure 6. pS1928 is required for increased vascular $\alpha1_C$ clustering in diabetes.
(**A**) Representative images of PLA puncta and summary puncta/µm² for $\alpha1_C$-$\alpha1_C$ interactions in sham and streptozotocin (STZ)-treated WT and S1928A arterial myocytes (WT sham n=40 cells from 6 mice; WT STZ n=34 cells from 6 mice; S1928A sham n=32 cells from 5 mice; S1928A STZ n=34 cells from 5 mice). Dashed lines represent the cells' footprints. (**B**) Representative super-resolution total internal reflection fluorescence (TIRF) images of arterial myocytes labeled for $\alpha1_C$ with 2 magnified areas showing cluster size and distribution in arterial myocytes from sham or STZ-treated WT and S1928A mice (scale bars=10 µm→1 µm→0.2 µm). (**C**) Amalgamated data for cluster size. (**D**) Representative nearest-neighbor interpolation map color-coded as a function of the number of neighbors within a 250 nm radius and frequency distribution data fitted to Gaussian curves (WT sham n=34 cells from 6 mice, WT STZ n=29 cells from 5 mice; S1928A sham n=41 cells from 5 mice, S1928A STZ n=34 cells from 5 mice). Data are mean±SEM. Significance was assessed with nested 2-way ANOVA with Bonferroni post-hoc test (**A**: P=0.0024, **C**: P=0.0079) and with extra sum-of-squares F test comparing centroids (**D**: WT P=1.1×10^{-5}, S1928A P=0.0706). P values within each panel and Table S11.

with S1928A sham cells (Figures 7A–7E, Figure S6B and S6C, Table S13 and S14). These results suggest that diabetes promotes pS1928-dependent $Ca_V1.2$ channel activity and cooperativity.

The *in vivo* implication of the spatial and gating remodeling of vascular $Ca_V1.2$ channels during diabetes and the involvement of pS1928 in this process were evaluated using Laser Speckle imaging as above. WT and S1928A mice were fitted with a cranial window to apply control or vasodilatory solutions to calculate the blood flow and myogenic tone in sham and STZ conditions. Results found an increase in myogenic tone with a decrease in blood flow in WT STZ mice compared with WT sham mice (Figures 7H and 7J, Table S14). Myogenic tone and blood flow in sham and STZ-treated S1928A mice were comparable to each other and the WT sham group (Figures 7H and 7J, Table S14). These results suggest that pS1928 contributes to HG-induced alterations in myogenic tone and blood flow in diabetic mice. Collectively, data indicate a key role for pS1928 in mediating increased $\alpha1_C$ subunit superclustering, $Ca_V1.2$ cooperativity, and myogenic tone leading to alterations in blood flow during diabetes.

DISCUSSION

Four key findings are described here. First, arterial myocytes from people with type 2 diabetes and type 1 diabetic mice, and WT cells exposed to HG showed reorganization of $\alpha1_C$ subunits into larger clusters (ie, "superclusters"). Second, the HG and diabetes-induced $\alpha1_C$ superclustering promoted increased frequency and strength of $Ca_V1.2$ cooperatively. Third, pS1928 is required for increased $\alpha1_C$ superclustering and $Ca_V1.2$ cooperativity upon HG and diabetes. Fourth, pS1928, through $\alpha1_C$ superclustering and $Ca_V1.2$ cooperativity, mediated enhanced cellular $[Ca^{2+}]_i$ and contractility, leading to concomitant alterations in myogenic tone and blood flow during HG and diabetes. These results highlight a previously unappreciated role for pS1928 in mediating the spatiotemporal remodeling of $Ca_V1.2$ channels to regulate vascular reactivity and blood flow during diabetic hyperglycemia. Results may lay the foundation for developing therapeutics with single amino acid accuracy that corrects $Ca_V1.2$ dysfunction during pathological conditions. This strategy may reduce the side effects of current options aimed at blocking channel activity rather than correcting aberrant channel function.

Nearly 30 years ago, Louis J. DeFelice proposed that L-type Ca^{2+} channels could organize into clusters of various sizes at the plasma membrane.[56] He further hypothesized that phosphorylation of one or more L-type Ca^{2+} channel subunits could induce "superclusters" and underlie functional alterations.[56] Despite these provocative ideas, supporting evidence is only starting to emerge. Accordingly, it was not until 2010 that $Ca_V1.2$ channels were conclusively shown to undergo cooperative gating and that this gating modality was boosted by stimuli that activated protein kinase C (PKC) in arterial myocytes.[3] Subsequently, it was found that β adrenergic activation in cardiomyocytes promoted a dynamic clustering of $\alpha1_C$ subunits.[8,11] Consistent with DeFelice ideas, results suggested that phosphorylation events could induce spatial rearrangement of L-type Ca^{2+} channel subunits, particularly $\alpha1_C$, which could facilitate $Ca_V1.2$ cooperative gating, but direct evidence was still missing. This study now provides compelling evidence supporting these hypotheses, directly correlating $\alpha1_C$ "superclusters" mediated by pS1928 during HG and diabetes with enhanced $Ca_V1.2$ cooperativity and current density in human and mouse arterial myocytes.

Supporting the statement above, pS1928 is increased in WT arterial lysates exposed to HG and lysates from people with diabetes and diabetic mice.[17,18] The HG and diabetes-induced increased pS1928 was mediated by activating a unique signaling complex stimulating the AKAP5/$P2Y_{11}$/AC5/PKA axis closely associated with the $\alpha1_C$ subunit.[17,18,24–27] Note that while other kinases (ie, PKC) may be activated in response to HG and diabetes, the effects of these stimuli on vascular $Ca_V1.2$ were mediated by PKA.[17,29] The increase in pS1928 to diabetic hyperglycemia was correlated with an increase in $\alpha1_C$ clustering in both human and mouse arterial myocytes (Figures 1, 3, and 6). These $\alpha1_C$ spatial remodeling coincided with an elevation in $Ca_V1.2$ activity and the frequency and strength of cooperative events (Figures 1, 2, and 7). Altered $\alpha1_C$ clustering and $Ca_V1.2$ cooperativity upon HG and diabetes were not observed in S1928A arterial myocytes (Figures 2, 3, 6, and 7). Yet, $Ca_V1.2$ cooperativity was increased by HG in S1700A arterial myocytes (Figure 4). These results confirm an essential role for $\alpha1_C$ pS1928 in the spatiotemporal control of vascular $Ca_V1.2$ channels during diabetic hyperglycemia. Results also raise the intriguing idea that $\alpha1_C$ phosphorylation by different stimuli or pathological conditions may lead to the formation of $\alpha1_C$ "superclusters" in arterial myocytes and other cells. Consistent with this possibility, it has been reported that mimicking phosphorylation in the neuronal $\alpha1_C$ subunit by replacing serine for glutamic acid at the 1928 position could promote the clustering of neuronal $\alpha1_C$ subunits.[57] Moreover, considering that S1928 has been shown to be phosphorylated by PKC and that PKC activation increases $Ca_V1.2$ cooperativity,[3,5,58,59] it is tempting to speculate that increased pS1928 may also lead to $\alpha1_C$ "superclustering" and enhanced $Ca_V1.2$ channel activity and cooperativity in response to angiotensin II/PKC signaling or hypertension. Thus, we proposed that phosphorylation-induced $\alpha1_C$ "superclustering" may be a general mechanism triggered by different stimuli or pathological conditions that may underlie alterations in $Ca_V1.2$ gating to modulate cellular response in arterial myocytes and perhaps other cell types.

ORIGINAL RESEARCH

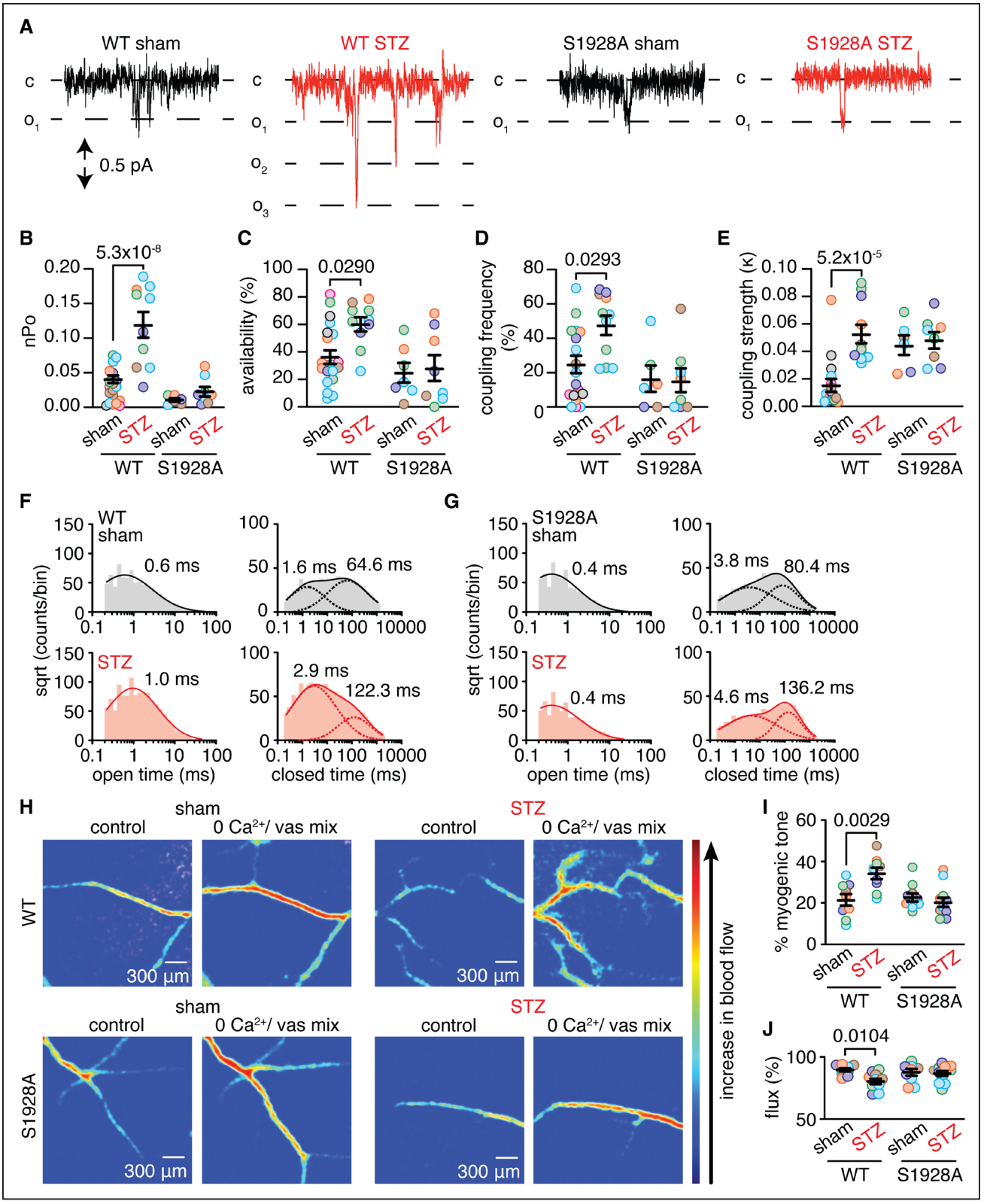

Figure 7. Functional changes in $Ca_V1.2$, arterial contractility, and blood flow during diabetes require pS1928.
A, Magnified areas of traces in S6B highlighting the closed (c) and unitary $Ca_V1.2$ opening levels (o_n) of representative cell-attached recordings from sham or STZ WT and S1928A arterial myocytes during a 2 s depolarizing step from −80 mV to −30 mV. Summary data of $Ca_V1.2$ (**B**) nPo, (**C**) availability, (**D**) coupling frequency, (**E**) coupling strength and (**F**, **G**) unitary events open and closed-time histograms obtained from WT and S1928A cells (WT sham n=19 cells from 7 mice; WT STZ n=10 cells from 5 mice; S1928A sham n=6 cells from 5 mice; S1928A STZ n=8 cells from 5 mice). **H**, Representative pseudo-colored blood flow images of sham and STZ-treated WT and S1928A cerebral pial arteries through a cranial window exposed to 10 mmol/L D-glu and 0 Ca^{2+} + vasodilatory mix. Summary data of (**I**) myogenic tone and (*Continued*)

Steady-state $\alpha1_C$ surface expression is maintained by dynamic endocytosis and (re)insertion of $\alpha1_C$ at the plasma membrane, including fusion and fission of $\alpha1_C$ containing vesicles.[60,61] The endocytosis and (re)insertion of $\alpha1_C$ can be influenced by phosphorylation events.[8,11,57] Recent work found that stimulating β adrenergic signaling in ventricular myocytes promoted the insertion of a pool of Rab4A/Rab11A positive $\alpha1_C$ containing vesicles to control $\alpha1_C$ plasma membrane abundance and clustering.[11] Moreover, enhanced neuronal $\alpha1_C$ clustering in neurons expressing a phosphomimetic construct for pS1928 (eg, S1928E) was associated with unknown mechanisms by which pS1928 boosts $\alpha1_C$ lateral diffusion and insertion.[57] Thus, it is likely that diabetic hyperglycemia-induced pS1928 promotes both lateral diffusion and the insertion of $\alpha1_C$ at the plasma membrane of arterial myocytes contributing to the formation of $\alpha1_C$ "superclusters." Consistent with these possibilities, both PLA and super-resolution data show an increase in $\alpha1_C$ cluster size and the number of neighboring $\alpha1_C$ clusters to another cluster at/near the plasma membrane of WT (and nondiabetic) arterial myocytes in response to diabetic hyperglycemia (Figures 1, 3, and 6). Yet, $\alpha1_C$ superclustering triggered by HG and diabetes was not observed in S1928A arterial myocytes. Indeed, super-resolution data suggest that $\alpha1_C$ cluster size and density are comparable in WT control/sham cells compared with S1928A control, sham, and STZ arterial myocytes. It is tempting to speculate that HG/diabetes-induced pS1928 promotes $\alpha1_C$ "superclustering" in arterial myocytes by enhancing $\alpha1_C$ (re)insertion rate at the plasma membrane by stimulating the recycling of $\alpha1_C$ from Rab25 positive recycling endosomes,[62] promoting the homotypic fusion of $\alpha1_C$ containing vesicles at/near plasma membrane regions,[61] or increasing the stochastic self-assembly of larger $\alpha1_C$ clusters.[63] Alternatively, HG/diabetes-induced pS1928 may also decrease the $\alpha1_C$ endocytosis rate.[57] Regardless of the mechanism, the results here strongly support the idea that pS1928 is essential for $\alpha1_C$ spatial remodeling in arterial myocytes during diabetic hyperglycemia.

The current model of $Ca_V1.2$ cooperativity suggests a physical interaction of 2 or more $\alpha1_C$ carboxy terminals mediated by Ca^{2+}•calmodulin (Ca^{2+}•CaM).[4,7] Data here now suggest that pS1928 may be a key initial step triggering $Ca_V1.2$ cooperativity. Accordingly, enhanced pS1928 can promote $\alpha1_C$ "superclustering" but also increase $Ca_V1.2$ activity and Ca^{2+} influx, thus triggering the Ca^{2+}•CaM-dependent bridging of $\alpha1_C$ carboxy terminals leading to enhanced $Ca_V1.2$ cooperativity. Consistent with these possibilities, data in this study correlate HG/diabetes-induced elevation in pS1928 with both $\alpha1_C$ "superclustering" and increased frequency/strength of $Ca_V1.2$ cooperativity in WT but not S1928A arterial myocytes (Figures 2, 3, 6, and 7). S1928A cells can still show some basal levels of $Ca_V1.2$ cooperativity. This may be caused by a pool of $\alpha1_C$ that could be tightly packed within a cluster. Activating one of the S1928A channels may allow enough Ca^{2+} entry, which could be "sensed" by a nearby CaM to initiate a weak bridging of $\alpha1_C$ carboxy terminals that contribute to basal $Ca_V1.2$ cooperativity. However, $Ca_V1.2$ cooperativity will not be augmented in S1928A arterial myocytes in response to a stimulus, such as diabetic hyperglycemia, because $\alpha1_C$ cannot form "superclusters" or increase $Ca_V1.2$ activity and Ca^{2+} influx due to the lack of pS1928. Thus, a double hit mechanism (pS1928 promotes $\alpha1_C$ superclusters and Ca^{2+} influx) may be required to further augment $Ca_V1.2$ activity and/or cooperative gating in response to diabetic hyperglycemia (and likely other stimuli). Another intriguing question is whether all $\alpha1_C$ subunits must be phosphorylated to stimulate $Ca_V1.2$ cooperative gating. This may not be entirely necessary as prior data suggest that $Ca_V1.2$ cooperativity is driven by the $Ca_V1.2$ channel with the highest open probability within the cluster.[6,45] In this scenario, an $\alpha1_C$ with increased pS1928 leading to higher $Ca_V1.2$ activity within the cluster may "hijack" a nearby unphosphorylated or basally phosphorylated $\alpha1_C$ to increase its activity and promote $Ca_V1.2$ cooperativity.

A major implication of pS1928-induced $\alpha1_C$ "superclustering" leading to enhanced $Ca_V1.2$ cooperativity is that it could amplify Ca^{2+} influx into cells, which may regulate a myriad of cellular responses, including contractility.[1,2,4] This study found that HG augmented the peak $[Ca^{2+}]_i$, which correlated with an ex vivo and in vivo increase in WT arterial myocyte contractility, resulting in enhanced myogenic tone and reduced blood flow (Figures 5 and 7). Similarly, diabetes increased cerebral artery myogenic tone and reduced blood flow in WT mice (Figure 7).[17] The alterations in arterial myocyte Ca^{2+} and contraction during diabetic hyperglycemia required pS1928 as HG/diabetes-induced changes in cellular Ca^{2+} and contractility, and in myogenic tone and blood flow were prevented in cells/arteries from S1928A mice (Figures 5 and 7). These results suggest that by controlling the spatiotemporal properties of $Ca_V1.2$, phosphorylation of $\alpha1_C$ at S1928 has a significant impact on the regulation of arterial myocyte contractility, myogenic tone, and blood flow during diabetic hyperglycemia. Blocking pS1928 may also help improve cardiovascular outcomes (eg, mean arterial

Figure 7 Continued. (**J**) flux (WT sham n=9 arteries from 5 mice; WT STZ n=9–10 arteries from 5 mice; S1928A sham n=10–11 arteries from 5 mice; 1928A STZ n=12 arteries from 5 mice). Data are mean±SEM. Significance was assessed with nested 2-way ANOVA with Bonferroni post-hoc test (**B**: *P*=0.0009, **C**: *P*=0.0318, **D**: *P*=0.0432, **E**: *P*=0.0109, **I**: *P*=0.0018, **J**: *P*=0.0432) and with extra sum-of-squares F test (**F**: WT *P*=0.0022; S1928A *P*=0.9917) for all conditions. Open/closed-time histograms were fitted with 1 or 2 Gaussian components, and centroids for open-time histograms were compared using an extra sum-of-squares F test (**F**: WT *P*=0.0022; **G**: S1928A *P*=0.9917). *P* values within each panel and Table S14.

pressure (MAP), heart rate, pulse pressure), as data show that genetic ablation of AKAP5, which prevents pS1928, ameliorates increased blood pressure during diabetes.[17,28] Thus, data provide a compelling link between pS1928, $\alpha 1_C$ "superclustering," $Ca_V1.2$ cooperativity, cellular function, and physiological response. It is intriguing to speculate that this vertical pathway is engaged in other tissues in health and disease.

In summary, data indicate that increased pS1928 underlies a spatiotemporal control of vascular $Ca_V1.2$ to modulate cellular $[Ca^{2+}]_i$ and contractility of arterial myocytes during HG and diabetes. The clinical and therapeutic implications of this mechanism are significant as they uncover a new mechanism underlying altered vascular reactivity during diabetic hyperglycemia and highlight the potential for the development of therapeutics that correct pathologically altered $Ca_V1.2$ function.

ARTICLE INFORMATION

Received June 5, 2022; revision received October 13, 2022; accepted October 27, 2022.

Affiliations

Department of Pharmacology, University of California Davis, Davis, CA (M.M.-A.B., V.A.F.-T., J.H., G.R.R., A.E.B., K.N.M.M., D.M.B., J.W.H., M.N.-C., M.F.N.). Department of Neurology, University of California Davis, Davis, CA (P.M.). Sasse Surgical Associates, Reno, NV (K.C.S.). Department of Physiology and Cell Biology, University of Nevada Reno, Reno, NV (S.M.W.). Department of Pharmacology, University of Washington, Seattle, WA (W.A.C.).

Acknowledgment

The authors thank Yumna Moustafa and Hanna M. Voorhees for technical support.

Sources of Funding

This work was supported by NIH grants R01HL121059 and R01HL161872, and UC MEXUS-CONACYT CN-19-147 (to MFN), and American Heart Association Postdoctoral Fellowship 830629 (to MM-AB). MN-C is a UC Davis CAMPOS Fellow.

Disclosures

None.

Supplemental Materials

Methods
Major Resources Table
Tables S1–S14
Figures S1–S6
References 3,5,7,17,18,23,26–28,30,31,33,35,36,40,41,46–49,52,55

REFERENCES

1. Hofmann F, Flockerzi V, Kahl S, Wegener JW. L-type CaV1.2 calcium channels: from in vitro findings to in vivo function. *Physiol Rev.* 2014;94:303–326. doi: 10.1152/physrev.00016.2013
2. Catterall WA. Voltage-gated calcium channels. *Cold Spring Harbor Perspect Biol.* 2011;3:a003947. doi: 10.1101/cshperspect.a003947
3. Navedo MF, Cheng EP, Yuan C, Votaw S, Molkentin JD, Scott JD, Santana LF. Increased coupled gating of L-type Ca2+ channels during hypertension and Timothy syndrome. *Circ Res.* 2010;106:748–756. doi: 10.1161/CIRCRESAHA.109.213363
4. Dixon RE, Navedo MF, Binder MD, Santana LF. Mechanisms and physiological implications of cooperative gating of clustered ion channels. *Physiol Rev.* 2022;102:1159–1210. doi: 10.1152/physrev.00022.2021
5. Navedo MF, Amberg GC, Votaw VS, Santana LF. Constitutively active L-type Ca^{2+} channels. *Proc Natl Acad Sci USA.* 2005;102:11112–11117. doi: 10.1073/pnas.0500360102
6. Dixon RE, Yuan C, Cheng EP, Navedo MF, Santana LF. Ca2+ signaling amplification by oligomerization of L-type Cav1.2 channels. *Proc Natl Acad Sci USA.* 2012;109:1749–1754. doi: 10.1073/pnas.1116731109
7. Dixon RE, Moreno CM, Yuan C, Opitz-Araya X, Binder MD, Navedo MF, Santana LF. Graded Ca(2)(+)/calmodulin-dependent coupling of voltage-gated CaV1.2 channels. *eLife.* 2015;4:e05608. doi: 10.7554/eLife.05608
8. Ito DW, Hannigan KI, Ghosh D, Xu B, Del Villar SG, Xiang YK, Dickson EJ, Navedo MF, Dixon RE. Beta-adrenergic-mediated dynamic augmentation of sarcolemmal CaV 1.2 clustering and co-operativity in ventricular myocytes. *J Physiol.* 2019;597:2139–2162. doi: 10.1113/JP277283
9. Vierra NC, Kirmiz M, van der List D, Santana LF, Trimmer JS. Kv2.1 mediates spatial and functional coupling of L-type calcium channels and ryanodine receptors in mammalian neurons. *eLife.* 2019;8:e49953. doi: 10.7554/eLife.49953
10. Jacquemet G, Baghirov H, Georgiadou M, Sihto H, Peuhu E, Cettour-Janet P, He T, Perala M, Kronqvist P, Joensuu H, et al. L-type calcium channels regulate filopodia stability and cancer cell invasion downstream of integrin signalling. *Nat Commun.* 2016;7:13297. doi: 10.1038/ncomms13297
11. Del Villar SG, Voelker TL, Westhoff M, Reddy GR, Spooner HC, Navedo MF, Dickson EJ, Dixon RE. Beta-Adrenergic control of sarcolemmal CaV1.2 abundance by small GTPase Rab proteins. *Proc Natl Acad Sci USA.* 2021;118:e2017937118. doi: 10.1073/pnas.2017937118
12. Amberg GC, Navedo MF, Nieves-Cintron M, Molkentin JD, Santana LF. Calcium sparklets regulate local and global calcium in murine arterial smooth muscle. *J Physiol.* 2007;579:187–201. doi: 10.1113/jphysiol.2006.124420
13. Knot HJ, Nelson MT. Regulation of arterial diameter and wall $[Ca^{2+}]$ in cerebral arteries of rat by membrane potential and intravascular pressure. *J Physiol.* 1998;508:199–209. doi: 10.1111/j.1469-7793.1998.199br.x
14. Tykocki NR, Boerman EM, Jackson WF. Smooth muscle ion channels and regulation of vascular tone in resistance arteries and arterioles. *Compr Physiol.* 2017;7:485–581. doi: 10.1002/cphy.c160011
15. Dixon RE. Nanoscale organization, regulation, and dynamic reorganization of cardiac calcium channels. *Front Physiol.* 2021;12:810408. doi: 10.3389/fphys.2021.810408
16. Liu G, Papa A, Katchman AN, Zakharov SI, Roybal D, Hennessey JA, Kushner J, Yang L, Chen BX, Kushnir A, et al. Mechanism of adrenergic CaV1.2 stimulation revealed by proximity proteomics. *Nature.* 2020;577:695–700. doi: 10.1038/s41586-020-1947-z
17. Nystoriak MA, Nieves-Cintron M, Patriarchi T, Buonarati OR, Prada MP, Morotti S, Grandi E, Fernandes JD, Forbush K, Hofmann F, et al. Ser1928 phosphorylation by PKA stimulates the L-type Ca2+ channel CaV1.2 and vasoconstriction during acute hyperglycemia and diabetes. *Sci Signaling.* 2017;10:eaaf9647. doi: 10.1126/scisignal.aaf9647
18. Prada MP, Syed AU, Buonarati OR, Reddy GR, Nystoriak MA, Ghosh D, Simo S, Sato D, Sasse KC, Ward SM, et al. A Gs-coupled purinergic receptor boosts Ca(2+) influx and vascular contractility during diabetic hyperglycemia. *eLife.* 2019;8:e42214. doi: 10.7554/eLife.42214
19. Qian H, Patriarchi T, Price JL, Matt L, Lee B, Nieves-Cintron M, Buonarati OR, Chowdhury D, Nanou E, Nystoriak MA, et al. Phosphorylation of Ser1928 mediates the enhanced activity of the L-type Ca2+ channel Cav1.2 by the beta2-adrenergic receptor in neurons. *Sci Signaling.* 2017;10:eaaf9659. doi: 10.1126/scisignal.aaf9659
20. Murphy JG, Sanderson JL, Gorski JA, Scott JD, Catterall WA, Sather WA, Dell'Acqua ML. AKAP-anchored PKA maintains neuronal L-type calcium channel activity and NFAT transcriptional signaling. *Cell reports.* 2014;7:1577–1588. doi: 10.1016/j.celrep.2014.04.027
21. De Jongh KS, Murphy BJ, Colvin AA, Hell JW, Takahashi M, Catterall WA. Specific phosphorylation of a site in the full-length form of the alpha 1 subunit of the cardiac L-type calcium channel by adenosine 3',5'- cyclic monophosphate-dependent protein kinase. *Biochemistry.* 1996;35:10392–10402. doi: 10.1021/bi953023c
22. Fu Y, Westenbroek RE, Scheuer T, Catterall WA. Phosphorylation sites required for regulation of cardiac calcium channels in the fight-or-flight response. *Proc Natl Acad Sci USA.* 2013;110:19621–19626. doi: 10.1073/pnas.1319421110
23. Fu Y, Westenbroek RE, Scheuer T, Catterall WA. Basal and beta-adrenergic regulation of the cardiac calcium channel CaV1.2 requires phosphorylation of serine 1700. *Proc Natl Acad Sci USA.* 2014;111:16598–16603. doi: 10.1073/pnas.1419129111
24. Martin-Aragon Baudel M, Espinosa-Tanguma R, Nieves-Cintron M, Navedo MF. Purinergic signaling during hyperglycemia in vascular smooth

muscle cells. *Front Endocrinol (Lausanne).* 2020;11:329. doi: 10.3389/fendo.2020.00329
25. Nieves-Cintron M, Flores-Tamez VA, Le T, Baudel MM, Navedo MF. Cellular and molecular effects of hyperglycemia on ion channels in vascular smooth muscle. *Cell Mol Life Sci.* 2021;78:31–61. doi: 10.1007/s00018-020-03582-z
26. Prada MP, Syed AU, Reddy GR, Martin-Aragon Baudel M, Flores-Tamez VA, Sasse KC, Ward SM, Sirish P, Chiamvimonvat N, Bartels P, et al. AKAP5 complex facilitates purinergic modulation of vascular L-type Ca(2+) channel CaV1.2. *Nat Commun.* 2020;11:5303. doi: 10.1038/s41467-020-18947-y
27. Syed AU, Reddy GR, Ghosh D, Prada MP, Nystoriak MA, Morotti S, Grandi E, Sirish P, Chiamvimonvat N, Hell JW, et al. Adenylyl cyclase 5-generated cAMP controls cerebral vascular reactivity during diabetic hyperglycemia. *J Clin Invest.* 2019;129:3140–3152. doi: 10.1172/JCI124705
28. Nystoriak MA, Nieves-Cintron M, Nygren PJ, Hinke SA, Nichols CB, Chen CY, Puglisi JL, Izu LT, Bers DM, Dell'acqua ML, et al. AKAP150 contributes to enhanced vascular tone by facilitating large-conductance Ca2+-activated K+ channel remodeling in hyperglycemia and diabetes mellitus. *Circ Res.* 2014;114:607–615. doi: 10.1161/CIRCRESAHA.114.302168
29. Navedo MF, Takeda Y, Nieves-Cintron M, Molkentin JD, Santana LF. Elevated Ca2+ sparklet activity during acute hyperglycemia and diabetes in cerebral arterial smooth muscle cells. *Am J Physiol Cell Physiol.* 2010;298:C211–C220. doi: 10.1152/ajpcell.00267.2009
30. Eisner DA. Pseudoreplication in physiology: more means less. *J Gen Physiol.* 2021;153:e202012826. doi: 10.1085/jgp.202012826
31. Nieves-Cintron M, Syed AU, Buonarati OR, Rigor RR, Nystoriak MA, Ghosh D, Sasse KC, Ward SM, Santana LF, Hell JW, et al. Impaired BKCa channel function in native vascular smooth muscle from humans with type 2 diabetes. *Sci Rep.* 2017;7:14058. doi: 10.1038/s41598-017-14565-9
32. Nystoriak MA, Nieves-Cintron M, Navedo MF. Capturing single L-type Ca(2+) channel function with optics. *Biochim Biophys Acta.* 2013;1833:1657–1664. doi: 10.1016/j.bbamcr.2012.10.027
33. Yue DT, Marban, E. Permeation in the dihydropyridine-sensitive calcium channel. Multi-ion occupancy but no anomalous mole-fraction effect between Ba2+ and Ca2+. *J Gen Physiol.* 1990;95:911–939. doi: 10.1085/jgp.95.5.911
34. Chung SH, Kennedy, RA. Coupled Markov chain model: characterization of membrane channel currents with multiple conductance sublevels as partially coupled elementary pores. *Math Biosci.* 1996;133:111–137. doi: 10.1016/0025-5564(95)00084-4
35. Buonarati OR, Henderson PB, Murphy GG, Horne MC, Hell JW. Proteolytic processing of the L-type Ca (2+) channel alpha 11.2 subunit in neurons. *F1000Res.* 2017;6:1166. doi: 10.12688/f1000research.11808.2
36. Davare MA, Horne MC, Hell JW. Protein phosphatase 2A is associated with class C L-type calcium channels (Cav1.2) and antagonizes channel phosphorylation by cAMP-dependent protein kinase. *J Biol Chem.* 2000;275:39710–39717. doi: 10.1074/jbc.m005462200
37. Rainbow RD, Hardy ME, Standen NB, Davies NW. Glucose reduces endothelin inhibition of voltage-gated potassium channels in rat arterial smooth muscle cells. *J Physiol.* 2006;575:833–844. doi: 10.1113/jphysiol.2006.114009
38. Nilsson J, Nilsson LM, Chen YW, Molkentin JD, Erlinge D, Gomez MF. High glucose activates nuclear factor of activated T cells in native vascular smooth muscle. *Arterioscler Thromb Vasc Biol.* 2006;26:794–800. doi: 10.1161/01.ATV.0000209513.00765.13
39. Hien TT, Turczynska KM, Dahan D, Ekman M, Grossi M, Sjogren J, Nilsson J, Braun T, Boettger T, Garcia-Vaz E, et al. Elevated glucose levels promote contractile and cytoskeletal gene expression in vascular smooth muscle via rho/protein kinase C and actin polymerization. *J Biol Chem.* 2016;291:3552–3568. doi: 10.1074/jbc.M115.654384
40. Lemke T, Welling A, Christel CJ, Blaich A, Bernhard D, Lenhardt P, Hofmann F, Moosmang S. Unchanged beta-adrenergic stimulation of cardiac L-type calcium channels in Ca v 1.2 phosphorylation site S1928A mutant mice. *J Biol Chem.* 2008;283:34738–34744. doi: 10.1074/jbc.M804981200
41. Navedo MF, Amberg GC, Westenbroek RE, Sinnegger-Brauns MJ, Catterall WA, Striessnig J, Santana LF. Ca(v)1.3 channels produce persistent calcium sparklets, but Ca(v)1.2 channels are responsible for sparklets in mouse arterial smooth muscle. *Am J Physiol Heart Circ Physiol.* 2007;293:H1359–H1370. doi: 10.1152/ajpheart.00450.2007
42. Barbagallo F, Xu B, Reddy GR, West T, Wang Q, Fu Q, Li M, Shi Q, Ginsburg KS, Ferrier W, et al. Genetically encoded biosensors reveal PKA hyperphosphorylation on the myofilaments in rabbit heart failure. *Circ Res.* 2016;119:931–943. doi: 10.1161/CIRCRESAHA.116.308964
43. DiPilato LM, Zhang J. The role of membrane microdomains in shaping beta2-adrenergic receptor-mediated cAMP dynamics. *Mol Biosyst.* 2009;5:832–837. doi: 10.1039/b823243a
44. Luo J, Deng ZL, Luo X, Tang N, Song WX, Chen J, Sharff KA, Luu HH, Haydon RC, Kinzler KW, et al. A protocol for rapid generation of recombinant adenoviruses using the AdEasy system. *Nat Protoc.* 2007;2:1236–1247. doi: 10.1038/nprot.2007.135
45. Cheng EP, Yuan C, Navedo MF, Dixon RE, Nieves-Cintron M, Scott JD, Santana LF. Restoration of normal L-type Ca2+ channel function during Timothy syndrome by ablation of an anchoring protein. *Circ Res.* 2011;109:255–261. doi: 10.1161/CIRCRESAHA.111.248252
46. Le T, Martin-Aragon Baudel M, Syed A, Singhrao N, Pan S, Flores-Tamez VA, Burns AE, Man KNM, Karey E, Hong J, et al. Secondhand smoke exposure impairs ion channel function and contractility of mesenteric arteries. *Function (Oxf).* 2021;2:zqab041. doi: 10.1093/function/zqab041
47. Vierra NC, O'Dwyer SC, Matsumoto C, Santana LF, Trimmer JS. Regulation of neuronal excitation-transcription coupling by Kv2.1-induced clustering of somatic L-type Ca(2+) channels at ER-PM junctions. *Proc Natl Acad Sci USA.* 2021;118:e2110094118. doi: 10.1073/pnas.2110094118
48. Ota K, Harada T, Otsubo K, Fujii A, Tsuchiya Y, Tanaka K, Okamoto I, Nakanishi Y. Visualization and quantitation of epidermal growth factor receptor homodimerization and activation with a proximity ligation assay. *Oncotarget.* 2017;8:72127–72132. doi: 10.18632/oncotarget.19552
49. Roberts RF, Wade-Martins R, Alegre-Abarrategui J. Direct visualization of alpha-synuclein oligomers reveals previously undetected pathology in Parkinson's disease brain. *Brain.* 2015;138:1642–1657. doi: 10.1093/brain/awv040
50. Fuller MD, Emrick MA, Sadilek M, Scheuer T, Catterall WA. Molecular mechanism of calcium channel regulation in the fight-or-flight response. *Sci Signaling.* 2010;3:ra70. doi: 10.1126/scisignal.2001152
51. Morotti S, Nieves-Cintron M, Nystoriak MA, Navedo MF, Grandi E. Predominant contribution of L-type Cav1.2 channel stimulation to impaired intracellular calcium and cerebral artery vasoconstriction in diabetic hyperglycemia. *Channels (Austin).* 2017;11:340–346. doi: 10.1080/19336950.2017.1293220
52. Otsu N. A threshold selection method from gray-level histograms. *IEEE Trans Syst Man Cybern.* 1979;9:62–66. doi: 10.1109/tsmc.1979.4310076
53. Creager MA, Luscher TF, Cosentino F, Beckman JA. Diabetes and vascular disease: pathophysiology, clinical consequences, and medical therapy: Part I. *Circulation.* 2003;108:1527–1532. doi: 10.1161/01.CIR.0000091257.27563.32
54. Brown A, Reynolds LR, Bruemmer D. Intensive glycemic control and cardiovascular disease: an update. *Nat Rev Cardiol.* 2010;7:369–375. doi: 10.1038/nrcardio.2010.35
55. Wu KK, Huan Y. Streptozotocin-induced diabetic models in mice and rats. *Curr Protoc Pharmacol.* 2008;Chapter 5:Unit 5 47. doi: 10.1002/0471141755.ph0547s40
56. DeFelice LJ. Molecular and biophysical view of the Ca channel: a hypothesis regarding oligomeric structure, channel clustering, and macroscopic current. *J Membr Biol.* 1993;133:191–202. doi: 10.1007/BF00232019
57. Folci A, Steinberger A, Lee B, Stanika R, Scheruebel S, Campiglio M, Ramprecht C, Pelzmann B, Hell JW, Obermair GJ, et al. Molecular mimicking of C-terminal phosphorylation tunes the surface dynamics of CaV1.2 calcium channels in hippocampal neurons. *J Biol Chem.* 2018;293:1040–1053. doi: 10.1074/jbc.M117.799585
58. Yang L, Liu G, Zakharov SI, Morrow JP, Rybin VO, Steinberg SF, Marx SO. Ser1928 is a common site for Cav1.2 phosphorylation by protein kinase C isoforms. *J Biol Chem.* 2005;280:207–214.
59. Raifman TK, Kumar P, Haase H, Klussmann E, Dascal N, Weiss S. Protein kinase C enhances plasma membrane expression of cardiac L-type calcium channel, CaV1.2. *Channels (Austin).* 2017;11:604–615. doi: 10.1080/19336950.2017.1369636
60. Conrad R, Stolting G, Hendriks J, Ruello G, Kortzak D, Jordan N, Gensch T, Hidalgo P. Rapid turnover of the cardiac L-Type CaV1.2 channel by endocytic recycling regulates its cell surface availability. *iScience.* 2018;7:1–15. doi: 10.1016/j.isci.2018.08.012
61. Ghosh D, Nieves-Cintron M, Tajada S, Brust-Mascher I, Horne MC, Hell JW, Dixon RE, Santana LF, Navedo MF. Dynamic L-type CaV1.2 channel trafficking facilitates CaV1.2 clustering and cooperative gating. *Biochim Biophys Acta Mol Cell Res.* 2018;1865:1341–1355. doi: 10.1016/j.bbamcr.2018.06.013
62. Bannister JP, Bulley S, Leo MD, Kidd MW, Jaggar JH. Rab25 influences functional Cav1.2 channel surface expression in arterial smooth muscle cells. *Am J Physiol Cell Physiol.* 2016;310:C885–C893. doi: 10.1152/ajpcell.00345.2015
63. Sato D, Hernandez-Hernandez G, Matsumoto C, Tajada S, Moreno CM, Dixon RE, O'Dwyer S, Navedo MF, Trimmer JS, Clancy CE, et al. A stochastic model of ion channel cluster formation in the plasma membrane. *J Gen Physiol.* 2019;151:1116–1134. doi: 10.1085/jgp.201912327